Experimental thermal evaluation of a bioclimatic light electric vehicle equipped with green roof and bio-based Phase Change Materials (PCM)

Amélie Danlos (amelie.danlos@lecnam.net)[1], Ivan Dobrev (ivan.dobrev@ensam.eu)[2], Fawaz Massouh (fawaz.massouh@ensam.eu)[2]

[1] Le Cnam, Arts et Métiers Institute of Technology, LIFSE, F-75013 Paris, France
[2] Arts et Métiers Institute of Technology, Le Cnam, LIFSE, F-75013 Paris, France

***Abstract* - Urban Heat Islands (UHIs) represent a critical environmental challenge in dense cities, intensified by thermal storage in parked automotive fleets. Exposed to solar radiation, vehicles overheat internally and reject heat into the urban canopy layer. In light electric micro-mobility, active air-conditioning is typically omitted due to energy and cost constraints. This paper presents a passive thermal control strategy developed by undergraduate apprentice students (Bachelor of Science in Engineering) from Le Cnam – GARAC for the UTAC Challenge 2026, a European student competition for future automotive solutions. The student project, embodied in a full-scale Citroën AMI demonstrator, combines two passive technologies to mitigate both vehicle-induced UHI effects and interior thermal discomfort: a lightweight green roof (Sedum vegetation) and interior bio-based Phase Change Materials (PCMs) composed of refined coconut oil encapsulated in natural fiber matrices. Tested in the thermal and aerodynamic wind tunnel of the Institut Aérotechnique du Cnam (IAT) under controlled solar irradiance and airflow, the green roof significantly reduces heat transfer into the cabin. Simultaneously, the bio-based PCMs attenuate cabin air temperature peaks via latent heat absorption at 24 °C. This study highlights the technical viability of passive thermal management while showcasing apprentice students' capacity to deliver innovative low-carbon transport solutions.**

***Keywords* - Electric vehicles, Thermal management, Phase Change Materials, Green Roof, Urban Heat Islands**

1. INTRODUCTION

Driven by climate change and rapid urbanization, cities increasingly suffer from the Urban Heat Island (UHI) effect, primary exacerbated by impervious, low-albedo construction materials and reduced evapotranspiration [1], [2]. While cool materials reduce air temperatures, they often elevate mean radiant temperatures and pedestrian thermal discomfort at street level [4]. Consequently, vegetated solutions such as green roofs offer a superior alternative by combining solar shading with evapotranspirative cooling [3, 5]. While buildings and pavement infrastructure have been widely investigated in urban microclimate literature, the thermal contribution of automotive fleets, and particularly stationary vehicles, has remained a largely under-addressed dynamic driver of local UHIs [6], [7]. In metropolitan areas, private vehicles spend over 95% of their operational lifespan parked on public streets or parking spaces [8]. This urban parking pressure is particularly acute in dense capitals such as Paris, where over 140,000 on-street parking spots occupied up to 75 hectares of public space, representing approximately 0.7% of the total city area including parks (or nearly 3% of all public street surfaces). Furthermore, parked resident vehicles represent a cumulative linear footprint equivalent to nearly 250 km of street space on a typical weekday [9], [10].

Composed of thin metallic and composite shells with high solar absorptance and low thermal inertia, parked vehicle bodies store minimal thermal mass and respond almost instantaneously to solar irradiance. This low thermal inertia triggers two immediate physical effects: a rapid rise of surface temperatures, frequently exceeding 60 °C to 70 °C within minutes of solar exposure, and an immediate conductive heat transfer across the thin shell, which is subsequently re-emitted into the cabin via convection and radiation [7], [11], [12].

To address these dual challenges: cabin overheating and urban heat island exacerbation without relying on active energy-consuming systems, the undergraduate apprentice student team selected a bioclimatic design philosophy inspired by low-carbon building engineering. Given the strict mass, volume, and financial constraints of light urban electric vehicles, the primary objective was to transpose proven passive building thermal management techniques into the automotive domain [3], [5]. Green roofs represent a proven nature-based solution that combines solar shading, mass buffering, and evapotranspirative cooling. While real-world transit bus pilots (e.g., *Garden on Wheels* in Singapore or *PhytoKinetic* in Spain) demonstrated mobile green roofs, peer-reviewed thermal data remains lacking. Installing an extensive vegetated layer on a vehicle roof absorbs solar flux and converts sensible heat into latent heat, passively shielding the cabin.

Complementing the radiative protection of the green roof, internal Phase Change Materials (PCMs) regulate air temperature fluctuations within the passenger compartment. PCMs store and release large amounts of thermal energy as latent heat during solid–liquid phase transitions within a target comfort range, offering a high-density passive thermal storage capacity [13], [14]. While commercial synthetic PCMs or paraffin waxes are often petroleum-derived and costly, organic bio-based PCMs, and specifically refined coconut oil, have emerged as an ideal low-cost, renewable alternative [15], [16]. Refined coconut oil exhibits exceptional thermophysical stability, a high latent heat of fusion (between 105-110 $J.g^{-1}$), and a phase transition temperature centered around 24 °C to 25 °C, which precisely matches the upper threshold of human thermal comfort in automotive enclosures [17]. This recent experimental study in automotive applications confirm that integrating coconut oil PCMs beneath vehicle roofs or

cabin liners can attenuate interior air temperature peaks by up to 15 °C during prolonged solar exposure.

To bridge this gap and provide rigorous empirical data on mobile passive cooling, the student team designed, fabricated, and instrumented a full-scale physical demonstrator named *CocoCombo*, based on a Citroën AMI micro-vehicle. This article presents the complete design of the bio-sourced dual cooling system combining a lightweight *Sedum* green roof with encapsulated refined coconut oil PCMs integrated inside the cabin.

Experimental measurements conducted in the aerodynamic and thermal wind tunnel at the Institut Aérotechnique (IAT, Cnam) will be presented nextto evaluate the thermal effectiveness of these combined passive solutions. This experimental investigation was submitted and defended by the student team at the UTAC 2026 Challenge under the *Cleaner Project* category. Although the project did not win an award at the competition, the experimental methodology, wind tunnel dataset, and physical insights detailed herein validate the technical feasibility and bioclimatic potential of converting urban micro-mobility into active cooling assets for warming cities.

2. MATERIALS AND PASSIVE COOLING SYSTEM DESIGN

Reducing this environmental impact inevitably requires accelerating the electrification of the automotive fleet [18]. However, the widespread adoption of electric vehicles remains limited, representing only 2.2% of the total operating fleet as of January 1, 2024 in France. The main identified barrier is the high acquisition cost, which renders these technologies inaccessible to low- and middle-income households. A strategic solution for decarbonizing the passenger car fleet lies in the introduction of more affordable light electric vehicles, as electric quadricycles. Limited to 45 km/h, they are perfectly suited to the daily mobility needs of the French population: studies indicate that 71% of daily journeys are under 10 km [19]. The Citroën AMI is a light urban electric quadricycle characterized by a simple structural design and expansive glass surfaces. While practical for urban micro-mobility, this architecture induces significant thermal fluctuations inside the cabin, leading notably to rapid overheating under solar radiation or fast cooling in cold weather.

A. Base vehicle platform: Citroën AMI

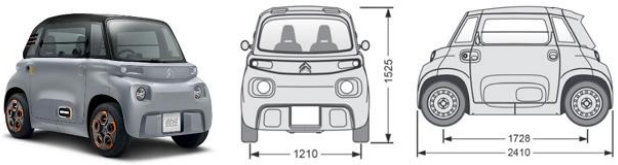


Fig. 1. Base vehicle platform: Citroën AMI.

The experimental platform is a Citroën AMI, an L6e electric light quadricycle featuring ultra-compact dimensions (2.41m length, 1.39m width, 1.52m height) and an unladen curb mass of 485kg including the battery (Fig. 1). Powered by a permanent magnet synchronous motor (6 kW nominal, 9 kW peak) and a 5.5 kWh (65kg) lithium-ion battery (80 Wh/km, 75km range), it recharges to 80% in 3h via a standard 230 V (8 A) domestic plug. Built for extreme mass and cost optimization, its architecture combines thin composite body panels over a tubular frame with extensive glazing, completely omitting active HVAC systems. While this minimizes vehicle weight and power consumption, it severely compromises thermal insulation. High solar transmittance and minimal roof thermal inertia lead to rapid interior overheating under solar exposure, making the vehicle an ideal baseline platform for evaluating passive, bio-sourced thermal management solutions.

B. Green roof architecture

To intercept solar flux before reaching the composite roof, an extensive green roof assembly was mounted on a custom frame (Fig. 2). The system relies on lightweight black polypropylene trays, which serve as modular containers housing the drainage and vegetative layers. Supplied by Paris Gazon (Marcoussis, France), the upper mat comprises a 30mm-thick pre-cultivated mixture of 8 to 10 *Sedum* varieties (*S. album*, *S. acre*, *S. reflexum*, etc.) selected for drought, heat, and frost resistance under automotive constraints.

Inside the trays, the plants are grown on a biodegradable coconut coir matrix acting as a lightweight binder and moisture reservoir (holding 8 to 10 times its weight in water). Beneath the substrate, the drainage layer uses porous expanded clay pebbles (about 300-400kg/m^3) rather than heavier pozzolan (about 800-100kg/m^3). To prevent bodywork staining, the drainage holes drilled into the trays are lined with a high-density polypropylene non-woven geotextile (about 60-80μm filtration), which retains fine particles without releasing tannins. Finally, the outer perimeters of the plastic trays are wrapped in bio-sourced hemp felt, providing a thermal break to prevent the dark polypropylene from conducting absorbed heat directly to the roof shell.

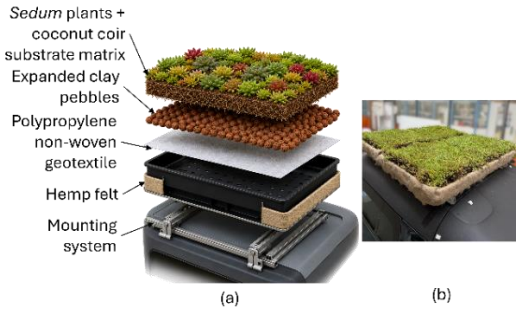


Fig. *2*. Structure of the green roof prototype: (a) Schematic breakdown of the green roof layers, from the Sedum canopy down to the mounting system, (b) Photography of the prototype integrated on a Citroën AMI.

For operational practicality and regulatory compliance, the green roof covers 1 m² using two modular recycled polypropylene trays (0.5 m² each). This two-part design enables easy manual installation and removal without hoisting equipment. The trays slide onto custom guide rails anchored directly to the vehicle's metallic chassis, secured by mechanical safety pins to withstand aerodynamic drag and vibrations. This mounting framework brings the total dry assembly mass to approximately $50kg$.

C. Bio-sourced PCM integration

Refined coconut oil was selected as a bio-sourced Phase

Change Material (PCM) to achieve passive thermal buffering without auxiliary electrical consumption. It satisfies human thermal comfort constraints with a solid-liquid phase transition between 24°C and 25°C, and a high latent heat of fusion ($\Delta H_f \approx 120\, kJ/kg$). Refining removes organic impurities, narrowing the melting range and guaranteeing long-term thermophysical stability. Sourcing from French overseas territories and processing in mainland France establishes a short-circuit domestic value chain that drastically reduces logistics emissions. Additionally, this organic medium is non-corrosive and non-toxic.

Liquid PCM macro-encapsulation relies on 2mm-thick Swedish sponge matrices (70% wood fibers, 30% recycled cotton) acting as a capillary retention network to prevent leakage and thermal stratification (Fig. 3). Once saturated, these matrices are vacuum-sealed inside biodegradable pouches to eliminate internal air resistance.

Mechanical integration against interior vehicle surfaces uses self-adhesive Velcro hook-and-loop strips paired with a high-tension natural hemp rope net. The assembly features 11 PCM panels ($20cm \times 18cm$) each, covering a total surface area of approximately 0.40m² distributed across the inner roof ceiling and interior door panels. The Velcro strips secure the flexible panels directly to these surfaces, while a hemp net provides secondary support pressing the roof panels firmly against the ceiling. Industrial hemp was selected over flax for its high dimensional stability under fluctuating cabin humidity, its local French sourcing, and its carbon sequestration capacity ($\approx 15t\ CO_2/ha$).



(a) (b)

Fig. 3. Prototype bio-sourced PCM panels: (a) individual coconut-oil-saturated sponge panel vacuum-sealed in a biodegradable pouch, and (b) panel layout integrated beneath the Citroën AMI roof shell.

Combining an exterior green roof for solar radiation shielding and evapotranspirative cooling with interior bio-sourced PCM panels for latent heat buffering creates a fully integrated, passive thermal management system. To quantify the actual thermal attenuation, heat flux reduction, and aerodynamic behavior of this coupled architecture under controlled environmental conditions, a full-scale experimental campaign was implemented.

3. EXPERIMENTAL METHODOLOGY AND MEASUREMENTS

Full-scale environmental testing was conducted in the S6 climatic thermal wind tunnel at the Institut Aérotechnique (IAT, Cnam) in Saint-Cyr-l'École, France.

A. Aerodynamic and thermal tunnel facility: IAT

The S6 facility is a specialized aerodynamic and climatic test chamber designed for full-vehicle thermal characterization, featuring a test section length of 17 m with flexible side walls. The test section cross-sectional area can be adjusted between $24m^2$ ($6m \times 4m$) and $36m^2$ ($6m \times 6m$), offering a contraction ratio ranging from 1.3 to 2.0. Airflow speeds up to $22\, m/s$ (approximately $80\, km/h$) are generated upstream by an array of 27 fans of $1.4m$ diameter, each rated at 28 kW. Environmental temperature regulation is supported by a 160 kW cooling unit and a 750 kW hot air generator capable of sustaining ambient test conditions up to 55 °C.

While the thermal chamber includes a 315kW chassis dynamometer for active powertrain testing, it was not utilized in this static investigation. However, the 3kW auxiliary ventilation bench was deployed for cabin heating evaluations. Overhead solar thermal loading is simulated via a gantry array equipped with 180 infrared lamps capable of delivering a uniform radiative flux up to $1.2\, kW/m^2$. Data acquisition is handled through a synchronized logging system monitoring up to 96 thermocouple channels simultaneously.

B. Measurements campaigns in thermal windtunnel

The experimental testing matrix was structured across two distinct single-day test sessions in the S6 wind tunnel. The first testing day evaluated the unmodified Citroën AMI to establish a comprehensive baseline reference. The second testing day focused on the prototype demonstrator, systematically testing configurations equipped either with the green roof alone or with the combined green roof and PCM system to isolate the thermal mitigation provided by each individual and coupled passive solution.

Connected directly to the wind tunnel data acquisition system, a network of 15 calibrated thermocouples (designated points A through N) recorded local temperatures at strategic locations both inside and outside the vehicle (Fig. 4). Sensor A monitored the overall climatic boundary condition within the S6 wind tunnel test section and was thus excluded from the vehicle structure layout. The remaining sensors mapped the thermal behaviour across the exterior skin, the roof assembly, and the passenger compartment.

External and structural instrumentation tracked surface and inter-layer temperatures, including the exterior roof glazing (point B), the outer door surface (point J), the green roof canopy at the center (point C) and edge (point D), the interface directly beneath the green roof and vehicle roof panel (point K), and the interior surface of the roof glazing under point B (point E).

Within the cabin, thermal monitoring was distributed across occupant-zone microclimate levels and interior panels. Head level and shoulder level for the driver were monitored at points F and G, respectively. Lower cabin positions included the interior left door opposite point J (point H) and the passenger footwell level (point I).

Finally, specialized roof-stack sensors evaluated the performance of the PCM ceiling panels and bare structural areas (Fig. 5). These comprised sensor L positioned underneath the PCM panels (glued to their interior side), sensor M located between the PCM layer and the vehicle roof panel, sensor N measuring the bare plastic roof panel directly in uninsulated and unglazed zones, and the sedum center sensor (point C). This comprehensive sensor

network enables a precise differential analysis of vertical heat transfer and internal microclimate attenuation.



Fig. 4. Thermocouple sensor positions (B-I) for internal cabin microclimate mapping and external roof stack thermal characterization on the Citroën AMI prototype. Sensor A monitors ambient air temperature within the S6 wind tunnel test section.

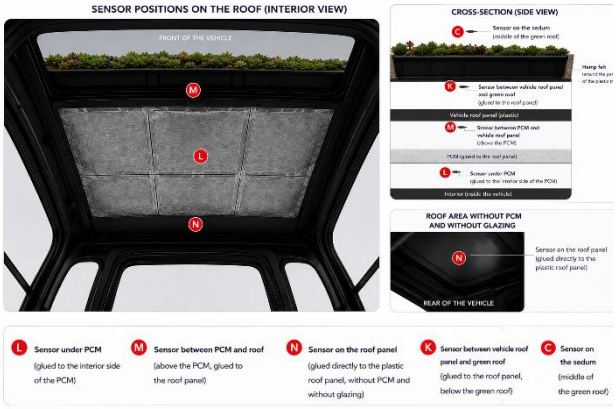


Fig. 5. Thermocouple locations (C, K-N) and cross-sectional view of the multi-layer roof structure integrating the green roof assembly and ceiling-mounted PCM panels.

Evaluating the reference case without thermal innovative solutions involved a total of twelve test conditions, which were systematically executed on the unmodified vehicle during the first testing day (Fig. 6 (a)). These baseline trials spanned varying airflow temperatures within the test section (from 25°C to 39°C), three discrete solar irradiance levels ($250\,W/m^2$, $600\,W/m^2$ and $1{,}000\,W/m^2$) and several internal ventilation states, including active cabin ventilation, inactive cabin fan, open windows, or closed windows.

The second testing day evaluated the prototype demonstrator (Fig. 6 (b)) across five distinct test cases, isolating the thermal mitigation provided by the green roof alone and in combination with the PCM installation. Throughout this second session, the cabin ventilation remained consistently inactive, and all vehicle windows were kept fully closed. For each configuration, continuous temperature data were logged for a duration of 30 minutes to capture steady-state thermal behaviour and transient accumulation. Operating conditions evaluated stationary parking exposure ($0\,km/h$ air velocity) against dynamic urban driving at $30\,km/h$, reflecting the standard speed limit in Paris. Solar flux levels were selected to mirror distinct seasonal and geographic scenarios: $600\,W/m^2$ corresponds to typical spring solar conditions in Paris when the sun is high in the sky, whereas $1{,}000\,W/m^2$ simulates extreme summer conditions characteristic of southern France while projecting future climate warming trends in northern regions.



(a) (b)

Fig. 6. Experimental test bench in the S6 wind tunnel showing (a) the baseline Citroën AMI reference case and (b) the passive cooling prototype demonstrator integrating the green roof and ceiling mounted PCM panels.

C. Complementary Outdoor Parking Bench for PCM Thermal Evaluation

To isolate the specific latent heat storage dynamics of the bio-sourced PCM ceiling panels, preliminary outdoor testing was conducted on a parking lot under natural spring solar radiation in April. Due to operational constraints and limited available testing time in the S6 wind tunnel facility, repeating dynamic thermal cycles inside the chamber was unfeasible. Wind tunnel testing requires complete re-solidification of the PCM matrix (achieved offline using refrigeration) to restore its latent cooling capacity after each full phase transition. Outdoor testing thus provided a practical method to measure PCM response under natural meteorological variations (Fig. 7).

The vehicle was initially parked in a shaded area to achieve a stabilized, uniform baseline interior air temperature of 21°C with solid-state PCM panels. The vehicle was then exposed to natural solar irradiance ranging between $700\,W/m^2$ and $800\,W/m^2$. With all windows fully closed and inactive ventilation inside the cabin. Because these trials were conducted under natural atmospheric conditions, radiative solar flux fluctuated dynamically with transient cloud cover. For this setup, the green roof assembly was omitted to evaluate only the interior PCM insulation layer.

Temperature evolution was recorded over a 1-hour period at 2-minute intervals using five dedicated thermocouple channels. Sensor 1 recorded the temperature underneath the PCM panel glued to the ceiling at the interface between the PCM and interior air, while sensor 2 tracked the air temperature at the passenger head level. Sensor 3 measured the external temperature directly on the outer roof surface. Sensor 4 was positioned underneath the roof shell in an uninsulated area where a PCM panel had been removed, putting the sensor in direct contact with the bare interior roof surface. Finally, sensor 5 monitored the outdoor ambient air temperature in direct sunlight, positioned approximately $1m$ away from the vehicle without any physical contact (Fig. 7).

Comparing sensors 1 and 4 isolates the direct contact

thermal attenuation provided by the bio-sourced PCM layer during solid-liquid phase transition, while the sensor 2 tracks the resulting microclimate stabilization within the occupant breather zone.

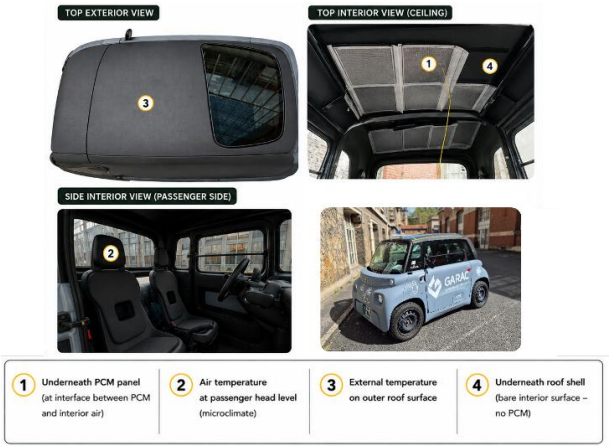


Fig. 7. Thermocouple locations (sensors 1 to 4) for standalone PCM performance evaluation under natural solar irradiance during parking lot testing. Sensor 5 is positioned 1 m away from the vehicle to record outdoor ambient air temperature in direct sunlight.

4. RESULTS AND DISCUSSION

A. Effects of PCM on thermal comfort

To assess the theoretical latent heat storage capacity of the interior ceiling configuration, a preliminary mass-energy balance was established prior to experimental testing. The PCM panels were fabricated using cellulose sponge cloths impregnated with refined coconut oil. In their dry state, the cloths exhibited an average mass of $8g$, a thickness of $2mm$, and dimensions of $20cm \times 18cm$. Upon saturation, the impregnated panels reached an average mass of $37g$ ($\pm 5g$) with an expanded thickness of $5mm$, yielding a net active PCM mass of approximately $29g$ of coconut oil per panel. Covering the interior roof and doors surface required a total of 11 panels, representing a total assembly mass of $407g$ containing $319g$ of active coconut oil. The total latent heat $Q_{L,PCM}$ absorbed during the solid-to-liquid phase transition is expressed as:

$$Q_{L,PCM} = m \times L_f \approx 38kJ \quad (1)$$

where m is the mass of the phase change material and L_f is its latent heat of fusion. Considering a latent heat of fusion $L_f = 110\ kJ/kg$ for refined coconut oil, the total theoretical energy absorption capacity of the ceiling installation is about $38kJ$. Although this thermal storage capability remains modest, it provides a functional proof-of-concept for passive thermal buffering within compact cabin architectures. Following these initial evaluations, increasing the volume and surface coverage of PCM panels throughout the interior compartment represents a straightforward avenue to enhance total latent heat capacity.

The temperature evolutions recorded during the outdoor parking exposure highlight both the severe greenhouse effect characteristic of the vehicle's geometry and the mitigation capacity provided by the bio-sourced PCM panels. As shown in Fig. 8, the temperature measured on the outer roof surface T_3 remains consistently lower than the interior temperature recorded directly beneath the uninsulated roof shell T_4. Solar radiation passing through the vehicle's expansive glass surfaces, combined with the lack of convective airflow in a closed stationary cabin, drives rapid heat accumulation. This pronounced greenhouse phenomenon leads to interior surface temperatures far exceeding ambient levels, demonstrating the necessity of thermal insulation and passive cooling strategies for such compact electric vehicles.

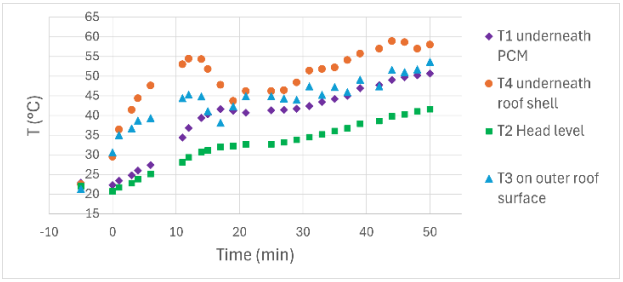


Fig. 8. Transient thermal response of the vehicle roof structure and interior cabin microclimate (T_1 to T_4) during a 50-minute outdoor parking test without the green roof, evaluated under natural solar loading to characterize standalone PCM performance.

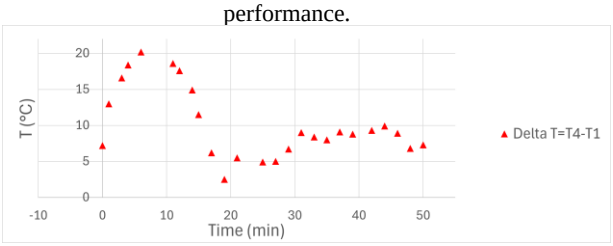


Fig. 9. Temperature difference ($\Delta T = T_4 - T_1$) to measure the effect of PCM under the roof during outdoor parking tests without green roof.

A comparison between the uninsulated roof contact sensor T_4 and the PCM-shielded interface sensor T_1 reveals the substantial thermal attenuation achieved by the ceiling layer. This thermal offset exhibit two distinct physical regimes:

- *Latent Heat Storage Phase:*

Approximately 3 minutes into the trial, as the interior roof environment reaches 24°C, corresponding to the melting point of the encapsulated coconut oil, the solid-to-liquid phase transition is triggered. During this phase change, the PCM absorbs significant thermal energy without a corresponding temperature rise, causing the divergence between T_4 and T_1 to widen sharply and reach a peak temperature difference of up to 20°C (Fig. 9).

- *Sensible Heat / Pure Thermal Resistance Phase:*

Once the PCM is fully liquefied and can no longer store heat latently, the panels continue to act as a physical thermal barrier. Even in its liquid state, the ceiling assembly maintains a steady thermal offset of 6°C relative to the bare roof surface due to its conductive insulation properties (Fig. 9).

These preliminary static findings establish the baseline latent efficiency of the PCM panels. Subsequent wind tunnel evaluations complement these results by isolating the coupled effects of forced convection and green roof shading on passenger thermal comfort.

To replicate the physical phase-change mechanisms observed during outdoor parking trials under fully

controlled boundary conditions, tests were conducted in the S6 climatic wind tunnel at an air temperature of 15°C and a solar irradiance of $600\,W/m^2$, simulating typical spring sunlight. Unlike the unconstrained outdoor setup, these trials incorporated the complete prototype demonstrator combining both the green roof assembly and interior PCM panels installed on the ceiling and side doors.

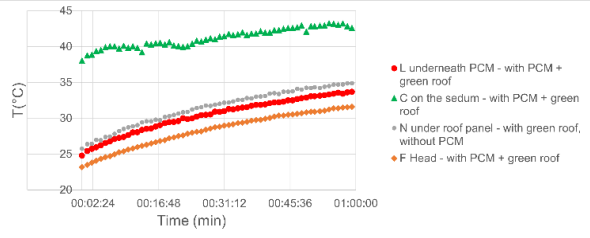


Fig. 10. Multi-layer roof temperature distribution under spring conditions (15°C, $600\,W/m^2$): thermal attenuation of green roof combined with PCM (L, C, F) vs. green roof alone (N).

Temperature evolution across the roof stack illustrates the interaction between the green roof and ceiling PCM panels (Fig. 10). Beneath the combined green roof and PCM assembly, the interface temperature directly under the PCM (sensor L) remains significantly lower than both the bare plastic roof shell without PCM (sensor N) and the temperature above the green roof, in the sedum (sensor C).

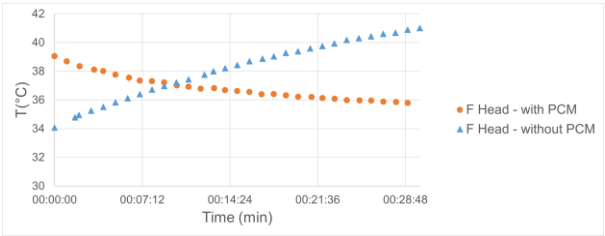


Fig. 11. Driver head-level air temperature ($sensor\ F$) during static parking ($0\,km/h$, 30°C ambient air, $1{,}000\,W/m^2$ solar flux): green roof alone vs. green roof + PCM.

By damping upward conductive and radiative gains, the ceiling PCM layer stabilizes local surface temperatures, preventing premature thermal saturation of the upper cabin air. Building upon the spring baseline performance, testing was extended to evaluate severe thermal stress conditions under a wind tunnel air temperature of 30°C and an extreme solar flux of $1000\,W/m^2$ during stationary parking ($0\,km/h$). To ensure a solid-state initial matrix despite the elevated wind tunnel chamber temperature, the PCM panels were pre-conditioned in a refrigerator prior to testing. Data logging commenced immediately after mounting the final PCM panel inside the cabin. Due to the about 10-minute handling duration required for panel installation within the warm environment, partial phase transition of the coconut oil had already initiated before $t = 0min$, though the active latent capacity was quite preserved. Monitoring air temperature at the driver head level (sensor F) highlights the specific contribution of the PCM layer when combined with the green roof (Fig. 11).

Without PCM (green roof alone), the head-level air temperature increases continuously over the 30-minute period, rising from 34°C to exceed 41°C due to persistent downward convective heating. In contrast, when interior PCM panels are integrated, latent heat absorption during phase change regulates internal air warming, stabilizing the driver head-level temperature at approximately 36°C in steady state. At thermal equilibrium, the interior PCM installation yields a net reduction of over 5°C in the driver breathing zone, demonstrating its capacity to mitigate localized thermal discomfort under high solar loads.

B. Effects of green roof on thermal comfort

A quantitative energy balance allows comparing the cooling performance of the $1m^2$ extensive *Sedum* green roof with the stock black ABS/polycarbonate composite plastic roof panel of the Citroën AMI across two representative operational scenarios:

- Extreme Summer Stress (30°C ambient air, $1{,}000\,W/m^2$ solar flux):

The stock unpainted black ABS/polycarbonate composite plastic roof panel, possessing a very low solar albedo ranging from 0.05 to 0.10, absorbs between 900 and $950\,W/m^2$ of incident radiation. Lacking latent dissipation pathways and thermal inertia, this energy is entirely converted into sensible heat. At thermal equilibrium under static conditions, heat loss partitions into natural convection ($\approx 280\,W/m^2$), sky thermal radiation ($\approx 290\,W/m^2$), and downward flux transferred into the vehicle ($\approx 330\,W/m^2$). This near-equal three-way distribution stems from the comparable magnitude of the heat transfer coefficients associated with natural convection on top of the horizontal panel, infrared radiation exchange with the sky, and overall downward heat transfer into the unconditioned cabin space. This thermal load drives surface temperature spikes above 65°C and turns the ceiling panel into a radiant heater, elevating internal air temperatures at driver head level (sensor F) up to 55°C or 58°C (and footwell air at sensor I up to 38°C or 42°C). In contrast, the *Sedum* canopy features a higher vegetative albedo about 0.20, absorbing $800\,W/m^2$ of net radiation (R_n). Under well-watered conditions, energy partitioning at the vegetated surface operates in a radiation-limited regime characterized by a Bowen ratio ($\beta = \frac{Q_S}{Q_L}$ with Q_S the sensible heat and Q_L the latent heat) of approximately 0.43. According to the surface energy balance:

$$R_n = Q_S + Q_L + G \tag{2}$$

Where G is the substrate heat flux (the conductive heat flux conducted downward into the substrate layer and towards the vehicle cabin). $G \approx 50\,W/m^2$ is considered negligible in this partitioning model, as it accounts for less than 6% of the net absorbed solar flux due to the low thermal conductivity and insulating property of the substrate layer.

The fraction of net absorbed flux converted into latent heat of vaporization is defined as:

$$\frac{Q_L}{R_n} = \frac{1}{1+\beta} \approx 0.70 \tag{3}$$

We then obtain $Q_L \approx 560\,W/m^2$. This mechanism dissipates up to $2\,MJ/h$ via a passive water evaporation rate of about $0.83\,L/h$ (considering the enthalpy of vaporization of water at 30°C equal to $L_v \approx 2.43\,MJ/kg$). Combined with the thermal mass and insulation of the substrate, the conductive heat flux G entering the cabin drops below $50\,W/m^2$ (an 85% reduction compared to the stock roof's $330\,W/m^2$), maintaining upper cabin air

temperatures (sensor F) close to ambient levels from 32°C to 35°C.

- Moderate Spring Conditions (17°C ambient air, $700\,W/m^2$ solar flux):

Under lower irradiance, the stock black roof panel still absorbs 630 to $665\,W/m^2$ of sensible heat, raising roof surface temperatures well above ambient air. Conversely, the green roof absorbs $560\,W/m^2$, with evapotranspiration converting roughly $390\,W/m^2$ into latent cooling ($Q_L \approx 1.4\,MJ/h$), corresponding to a passive water consumption of about $0.58\,L/h$and effectively mitigating cabin heat buildup. Under these moderate spring conditions, the residual conductive flux transmitted through the vegetated assembly drops below $30\,W/m^2$, maintaining upper cabin air temperatures (sensor F) between 19°C and 21°C (compared to 32°C or 36°C for the stock black roof panel).

While 1D conduction models focus on ceiling flux, predicting upper cabin air temperatures (sensor F) requires accounting for direct solar gains through vertical and sloped glazing (> 50% of upper bodywork). Shortwave radiation entering unshaded windows (from 75% to 85 % transmittance) is absorbed by dark interior surfaces and re-emitted as longwave Infrared. Trapped by the greenhouse effect, this thermal load generates a convective plume that stratifies buoyant hot air beneath the ceiling:

- *Spring Validation (17°C ambient air):*

Direct window gains ($\approx 700 - 800W$) dominate cabin heating over residual green roof conduction ($G < 30\,W/m^2$), driving sensor F readings to 35°C (explaining the gap with the isolated 1D roof prediction of about 20°C and the 32°C obtained at head level on Fig. 10).

- *Summer Impact (30°C ambient air):*

Window radiation adds about 1.1 kW of internal load. Eliminating ceiling conductive gain with the green roof reduces sensor F air temperature from about 58°C (stock roof) down to about 42°C. These theoretical energy balance calculations are well corroborated by our thermal wind tunnel measurements under static parked conditions, which recorded air temperatures stabilizing around 40°C at driver head level (sensor F) under extreme summer stress.

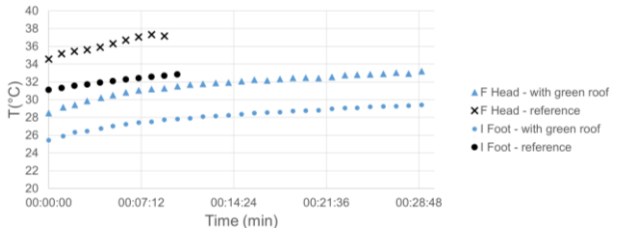


Fig. 12. Vertical air temperature at head (F) and footwell (I) levels during urban driving ($30\,km/h$, 30°C, $1{,}000\,W/m^2$): baseline vs. green roof prototype.

To isolate the passive cooling capabilities of the extensive green roof, tests were conducted at dynamic urban driving speed ($30\,km/h$) under 30°C ambient air temperature and $1{,}000\,W/m^2$ solar irradiance, without interior PCM activation. Fig. 12 compares internal temperatures at head level (sensor F) and footwell level (sensor I) between the green-roof-equipped prototype and the stock baseline vehicle. Although data logging for the reference case was restricted to a shorter duration, both configurations exhibit a persistent vertical thermal gradient of approximately 4°C between the occupant breathing zone and the lower footwell. Standard thermal comfort criteria dictate that vertical air temperature differences between head and feet should remain below 3°C to avoid localized discomfort. While the green roof lowers absolute temperatures at both vertical stations by mitigating overall heat flux, it does not alter this head-to-foot thermal disparity.

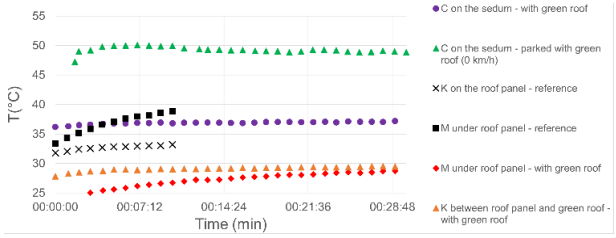


Fig. 13. Multi-layer roof stack temperature evolution during dynamic ($30\,km/h$) and static ($0\,km/h$) tests conditions (30°C, $1{,}000\,W/m^2$): stock roof vs. green roof layers.

Fig. 13 details the layer-by-layer heat transfer across the roof stack under dynamic ($30\,km/h$) and stationary ($0\,km/h$) conditions. In the stock baseline vehicle, interior ceiling temperatures (sensor M) consistently exceed external surface levels (sensor K) due to severe solar heat trapping inside the uninsulated cabin. Integrating the green roof reverses this trend, significantly lowering temperatures across the roof stack and inside the upper cabin. Forced convection at $30\,km/h$ substantially enhances cooling: canopy surface temperatures on the Sedum layer (sensor C) drop by 14°C compared to the stationary parking state ($0\,km/h$). However, this strong airflow at $30\,km/h$ also causes the temperature underneath the green roof tray (sensor K) to equalize gradually with the interior ceiling temperature (sensor M). This thermal equalization indicates that convective airflow through the air gap partially dissipates the evapotranspirative cooling before it fully penetrates the cabin. To maximize internal thermal benefits, positioning the green roof assembly closer to the vehicle roof panel would reduce convective air losses and improve conductive heat removal.

5. CONCLUSION

This study presents a novel passive thermal management proof-of-concept for ultra-compact urban electric vehicles, developed by a team of eight undergraduate apprentice engineers from Cnam and GARAC as part of the UTAC 2026 Challenge (Free Cleaner project category). As climate change accelerates the frequency and intensity of summer heatwaves in urban areas, mitigating internal vehicle heat gain without over-relying on energy-intensive air conditioning becomes a critical priority. Mobile green roofs offer a double benefit: protecting the vehicle cabin while contributing to the reduction of Urban Heat Islands (UHIs) across dense city environments. By combining an extensive bio-receptive green roof with ceiling and door panels of bio-sourced Phase Change Material (PCM), the project addresses severe thermal discomfort and energy penalties in minimalist electric architectures.

From an economic perspective, this combined bio-sourced strategy offers an exceptionally low-cost

alternative to active refrigeration. The entire extensive green roof assembly was implemented for €300, while the interior macro-encapsulated PCM system was fabricated for €115. Totaling less than €420, this approach demonstrates that significant interior thermal buffering can be achieved at a fraction of the cost, mass, and complexity of conventional active air conditioning systems.

Experimental characterization, conducted both in natural outdoor environments and inside the IAT S6 thermal wind tunnel, demonstrates the complementary physics of these two passive mechanisms. Under extreme stationary solar exposure (30°C, $1{,}000\,W/m^2$), interior PCM panels suppress secondary radiative heating, stabilizing driver head-level temperature at approximately 36°C and achieving a net reduction of over 5°C compared to the green-roof-only baseline. Under dynamic driving conditions ($30\,km/h$), forced convection enhances cooling effect, reducing the *Sedum* canopy surface temperature by 14°C relative to the static state. While operational time constraints in the wind tunnel and thermal cycling recovery limits of the PCM matrix restricted the scope of steady-state repetitions, these initial findings validate the viability of dual passive coupling without active auxiliary energy consumption. Several key perspectives are outlined to advance this research:

- *Thermal Optimization (Cascade Melting):*

Implementing a multi-stage PCM architecture with staggered melting points (spanning 22°C to 28°C) to extend latent heat absorption capacity over broader temperature ranges and prevent premature liquid saturation under prolonged solar exposure.

- *Structural Safety and Dynamic Stability:*

Conducting crashworthiness and emergency braking assessments to evaluate panel mechanical integrity during impacts with pedestrians or cyclists. Furthermore, detailed dynamic modelling will address the elevation of the vehicle's center of gravity caused by the additional top mass (60 kg at a height of 1.50 m), optimizing mass distribution to mitigate lateral load transfer during evasive maneuvers.

Ultimately, this initiative highlights how hands-on student projects provide an agile platform to test bold, creative technical solutions, offering concrete reasons for optimism regarding the future of sustainable urban mobility.

Acknowledgment

The author would like to express her sincere gratitude to the undergraduate apprentice engineers from Cnam and GARAC whose dedicated teamwork and experimental contributions made this project possible. Special thanks are extended to the 2025-2026 team: Harold Bottin, Théo Gaillard, Etienne Poirier, Victor Pontoizeau, Robin Blee, Kenan Efe Kabali, Nahel Nebati, and Mathis Peyrounin for their involvement in developing the prototype demonstrator and conducting the PCM and green roof trials. The author also acknowledges the 2024-2025 student team: Ankur Banik, Adrien Claudez, Nicolas Gobin-Viacava, and Théo Polidano for their foundational work in collecting the baseline benchmark data on the reference vehicle.

The authors also acknowledge the joint academic support of the Institut Aérotechnique (IAT) of Saint-Cyr-l'Ecole, as well as SIA and UTAC for organizing the Challenge UTAC.

REFERENCES

[1] T. R. Oke, 'The energetic basis of the urban heat island', *Quarterly Journal of the Royal Meteorological Society*, vol. 108, no. 455, pp. 1–24, 1982, doi: 10.1002/qj.49710845502.

[2] J. A. Voogt and T. R. Oke, 'Thermal remote sensing of urban climates', *Remote Sensing of Environment*, vol. 86, no. 3, pp. 370–384, Aug. 2003, doi: 10.1016/S0034-4257(03)00079-8.

[3] M. Santamouris, 'Cooling the cities – A review of reflective and green roof mitigation technologies to fight heat island and improve comfort in urban environments', *Solar Energy*, vol. 103, pp. 682–703, May 2014, doi: 10.1016/j.solener.2012.07.003.

[4] E. Erell, D. Pearlmutter, D. Boneh, and P. B. Kutiel, 'Effect of high-albedo materials on pedestrian heat stress in urban street canyons', *Urban Climate*, vol. 10, pp. 367–386, Dec. 2014, doi: 10.1016/j.uclim.2013.10.005.

[5] A. B. Besir and E. Cuce, 'Green roofs and facades: A comprehensive review', *Renewable and Sustainable Energy Reviews*, vol. 82, pp. 915–939, Feb. 2018, doi: 10.1016/j.rser.2017.09.106.

[6] M. Matias, G. Mills, T. Silva, C. Girotti, and A. Lopes, 'The underestimated impact of parked cars in urban warming.', *City and Environment Interactions*, vol. 28, p. 100232, Dec. 2025, doi: 10.1016/j.cacint.2025.100232.

[7] M. Matias, C. Girotti, T. Silva, G. Mills, L. F. Kowalski, and A. Lopes, 'Thermal Impacts of Stationary Vehicles on Urban Microclimates: Insights from Field Measurements and Exploratory 3D Modelling', *Atmosphere*, vol. 17, no. 4, p. 390, Apr. 2026, doi: 10.3390/atmos17040390.

[8] D. Shoup, 'The High Cost of Free Parking', *Journal of Planning Education and Research*, vol. 17, pp.3-20, 1997.

[9] APUR, 'Évolution du stationnement et nouveaux usages de l'espace public'. Accessed: June 22, 2026. [Online]. Available: https://www.apur.org/fr/mobilites-espace-public/usages-espace-public/evolution-stationnement-usages-espace-public

[10] PARIS, 'Paris réforme son stationnement'. Accessed: June 22, 2026. [Online]. Available: https://www.paris.fr/pages/paris-reforme-son-stationnement-17981

[11] Y. Zhang, Z. Li, S. Liu, G. Wang, and H. Chang, 'A Study of Passenger Car Cabin Pre-Ventilation under the Sun', *Energies*, vol. 16, no. 20, p. 7154, Jan. 2023, doi: 10.3390/en16207154.

[12] R. Levinson, H. Pan, G. Ban-Weiss, P. Rosado, R. Paolini, and H. Akbari, 'Potential benefits of solar reflective car shells: Cooler cabins, fuel savings and emission reductions', *Applied Energy*, vol. 88, no. 12, pp. 4343–4357, Dec. 2011, doi: 10.1016/j.apenergy.2011.05.006.

[13] A. Afzal *et al.*, 'Human thermal comfort in passenger vehicles using an organic phase change material– an experimental investigation, neural network modelling, and optimization', *Building and Environment*, vol. 180, p. 107012, Aug. 2020, doi: 10.1016/j.buildenv.2020.107012.

[14] S. Wonorahardjo, I. M. Sutjahja, D. Kurnia, Z. Fahmi, and W. A. Putri, 'Potential of Thermal Energy Storage Using Coconut Oil for Air Temperature Control', *Buildings*, vol. 8, no. 8, p. 95, Aug. 2018, doi: 10.3390/buildings8080095.

[15] A. O. Silalahi, N. Sukmawati, I. M. Sutjahja, D. Kurnia, and S. Wonorahardjo, 'Thermophysical Parameters of Organic PCM Coconut Oil from T-History Method and Its Potential as Thermal Energy Storage in Indonesia', *IOP Conf. Ser.: Mater. Sci. Eng.*, vol. 214, no. 1, p. 012034, Jul. 2017, doi: 10.1088/1757-899X/214/1/012034.

[16] E. Paroutoglou, P. Fojan, L. Gurevich, and A. Afshari, 'Thermal Properties of Novel Phase-Change Materials Based on Tamanu and Coconut Oil Encapsulated in Electrospun Fiber Matrices', *Sustainability*, vol. 14, no. 12, p. 7432, Jan. 2022, doi: 10.3390/su14127432.

[17] C. A. Saleel, M. A. Mujeebu, and S. Algarni, 'Coconut oil as phase change material to maintain thermal comfort in passenger vehicles', *J Therm Anal Calorim*, vol. 136, no. 2, pp. 629–636, Apr. 2019, doi: 10.1007/s10973-018-7676-y.

[18] Assemblée nationale, "Rendre les véhicules électriques accessibles sur tout le territoire," in *Avis fait au nom de la commission des finances sur le projet de loi de finances pour 2025*, 2024. Accessed: June 22, 2026. [Online]. Available: https://www.assemblee-nationale.fr/dyn/opendata/AVISANR5L17B0486-tIV.html.

[19] SDES, "Les pratiques de mobilité des Français varient selon la densité des territoires," Ministère de la Transition écologique, Paris,

France, 2024. Accessed: June 22, 2026. [Online]. Available: https://www.statistiques.developpement-durable.gouv.fr/les-pratiques-de-mobilite-des-francais-varient-selon-la-densite-des-territoires